Acta Materialia 105 (2016) 176–181

Contents lists available at ScienceDirect

Acta Materialia

journal homepage: www.elsevier.com/locate/actamat

Full length article

Direct measure of giant magnetocaloric entropy contributions in Ni–Mn–In

Jing-Han Chen [a, *], Nickolaus M. Bruno [b], Ibrahim Karaman [b, c], Yujin Huang [d], Jianguo Li [d], Joseph H. Ross Jr. [a, c]

[a] Department of Physics and Astronomy, Texas A&M University, College Station, 77843, TX, USA
[b] Department of Mechanical Engineering, Texas A&M University, College Station, 77843, TX, USA
[c] Department of Materials Science and Engineering, Texas A&M University, College Station, 77843, TX, USA
[d] School of Materials Science and Engineering, Shanghai Jiaotong University, Shanghai, 200240, China

ARTICLE INFO

Article history:
Received 24 September 2015
Received in revised form
26 November 2015
Accepted 28 November 2015
Available online xxx

Keywords:
Magnetocaloric effect
Heusler alloys
Entropy
Calorimetry

ABSTRACT

Off-stoichiometric alloys based on Ni_2MnIn have drawn attention due to the coupled first order magnetic and structural transformations, and the large magnetocaloric entropy associated with the transformations. Here we describe calorimetric and magnetic studies of four compositions. The results provide a direct measure of entropy change contributions at low temperatures as well as at the first-order phase transitions. Thereby we determine the maximum possible field-induced entropy change corresponding to the giant magnetocaloric effect. We find a large excess entropy change above that of the magnetic moments, but only in compositions with no ferromagnetic order in the high-temperature austenite phase. Furthermore, a molecular field model corresponding to magnetic order in the low-temperature phases is in good agreement, giving an entropy contribution nearly independent of composition, despite significant differences in overall magnetic response of these materials.

1. Introduction

The magnetocaloric effect (MCE) is an intrinsic thermodynamic property of magnetic solids, manifested as an adiabatic temperature change or an isothermal entropy change due to application of a magnetic field. Materials showing a large MCE have been a source of growing interest because of their potential for environmentally friendly and energy efficient replacement of vapor-compression refrigeration [1,2]. Giant MCE is based on a first-order phase transition and has been observed in materials including the Ni–Mn based Heusler alloys [3–10] discussed here, as well as $Gd_5Si_{2-x}Ge_x$ materials [11], MnAs-based compounds [12–14] and $LaFe_{13-x}Si_x$ related compounds [15,16]. Ni–Mn–In alloys exhibit a large response, and have magnetic and structural properties that depend very sensitively on the composition and preparation conditions [17]. In this report, we examine four different Ni–Mn–In compositions to better understand the relationship of magnetic and structural properties vs. composition.

One of the common physical quantities used to characterize MCE materials is the magnetic field-induced isothermal entropy change. This quantity can be explored both by calorimetry and indirectly through magnetization [18–24]. As Fig. 1 illustrates, the entropy change intrinsic to the first-order transformation is the maximum possible field-induced entropy change (ΔS_{max}), which can be explored directly through calorimetry in zero field even though this quantity may not be necessarily accessible through measurements of ΔS in available fields. Aside from the practical importance there is considerable interest in understanding the underlying physical processes that contribute to this behavior [25–27]. In this report, we examine the various contributions to the total entropy in several Ni–Mn–In alloys, including an examination of the contributions to ΔS_{max}.

We describe results based on magnetic and calorimetric measurements. These results provide a consistent picture of the magnetic behavior of the low temperature (martensite) phases, dominated by magnetic order based on interacting local moments. Furthermore, the entropy jump at the transformation, equivalent to ΔS_{max}, is shown to be very sensitive to the composition. Relative to the magnetic contribution, a significant excess is found in compositions exhibiting magnetic order in the austenite (high-

* Corresponding author.
E-mail address: jhchen@tamu.edu (J.-H. Chen).

http://dx.doi.org/10.1016/j.actamat.2015.11.053
1359-6454/

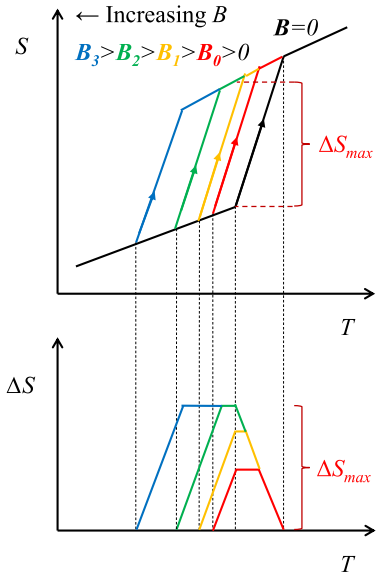

Fig. 1. Schematic representation of the total entropy in different applied fields along with the field-induced isothermal entropy change (lower plot) for inverse MCE materials in the vicinity of a first-order phase transition.

temperature) phase, implying an apparent magnetoelastic coupling tied to the magnetic order of the austenite.

2. Experiment

2.1. Sample preparation

Bulk polycrystalline Ni–Mn–In alloys were prepared using arc melting in a protective argon atmosphere from 99.9% pure constituents. This includes the sample used for measurements reported previously [23] along with 3 other compositions prepared by identical methods. The samples were homogenized at 1173 K for 24 h under argon atmosphere and then quenched to room temperature in water. These heat treating conditions were found to result in sharp first-order transitions and small thermal hysteresis. Since the alloy was quenched above the order disorder temperature [28], *B*2 crystallographic symmetry will dominate in these samples with Ni on one sublattice and Mn and In randomly occupying the other, rather than the Heusler-type $L2_1$ ordering obtained at lower temperatures.

Electron microprobe measurements were carried out using wavelength dispersive spectroscopy methods on a Cameca SX50, equipped with four wavelength-dispersive x-ray spectrometers. Among the four Ni–Mn–In compositions, the final compositions were found to be $Ni_{49.54}Mn_{36.12}In_{14.34}$ (the sample used in the previous report [23]), $Ni_{49.9}Mn_{35.7}In_{14.4}$, $Ni_{49.53}Mn_{35.22}In_{15.22}$ and $Ni_{47.22}Mn_{38.45}In_{14.33}$. We label these samples as A, B, C and D, respectively, as shown in Table 1.

Table 1
Ni–Mn–In compositions (in at. %) and the corresponding experimental results. J and T_c are from the high-temperature Curie–Weiss fits, and T_{mh} (martensitic transition temperature) is the maximum position of the specific heat measured while heating.

Label	WDS composition	J	T_c(K)	T_{mh}(K)	γ(J/mole K^2)	θ_D(K)
A	$Ni_{49.54}Mn_{36.12}In_{14.34}$	2.00	292	347	0.0124	315
B	$Ni_{49.88}Mn_{35.70}In_{14.42}$	1.99	310	333	0.0128	318
C	$Ni_{49.53}Mn_{35.22}In_{15.22}$	2.00	323	299	0.0117	316
D	$Ni_{47.22}Mn_{38.45}In_{14.33}$	2.00	298	257	0.0163	316

2.2. Measurement methods

Iso-field magnetic measurements were carried out using a Quantum Design Magnetic Property Measurement System. The temperature-dependent results in 0.05 T shown in Fig. 2 include prominent features due to the first-order martensitic phase transitions falling between 200 and 350 K. As shown below, the smaller responses in the A and B compositions come about since the austenite (high-temperature) phase for these cases are paramagnetic rather than ferromagnetic.

Besides the magnetic measurements, calorimetric measurements were performed using a Physical Property Measurement System manufactured by Quantum Design. Samples were affixed using a thin layer of grease to the small sample platform of a standard puck, with the platform connected by thin wires to the body of the puck. For temperatures away from the structural transition, the so-called 2-τ method [29] was used. Since this method is not valid for a first order transition, we used the modified method described previously [23], by which we obtain results consistent with the 2-τ method outside the transition temperature region.

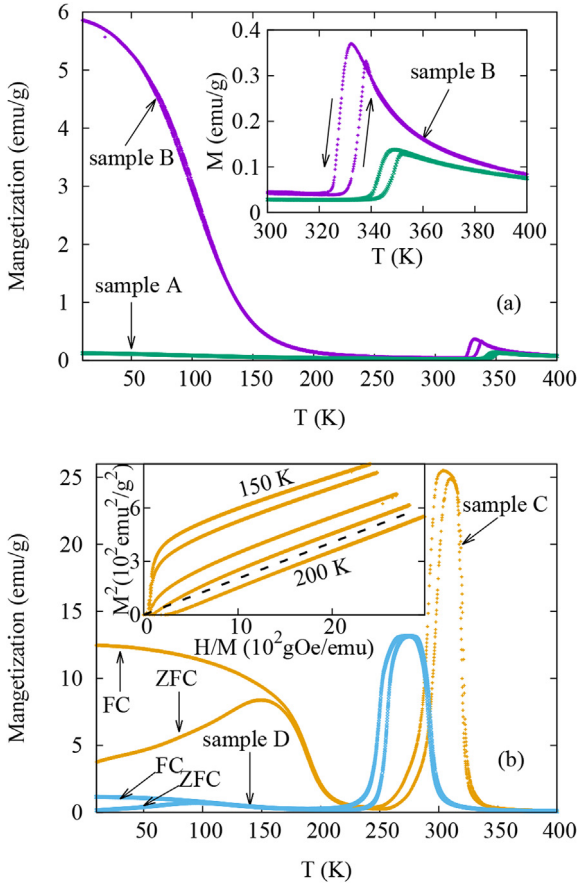

Fig. 2. Temperature dependence of the magnetization for the Ni–Mn–In samples at 0.05 T, including (a) A and B samples and (b) C and D samples. All data include results for both heating and cooling processes, as shown by arrows for sample B in the inset of the upper figure. For samples C and D, the low-temperature bifurcation corresponds to field-cooled (FC) and zero-field cooled (ZFC) measurements as shown. An Arrott plot for sample C is shown in the lower inset. These curves were measured at temperatures 150, 160, 180, 190, and 200 K. The dashed line extending through the origin corresponds to 194 K, the approximate position of the second order transformation as described in the text.